

Article

Regression Equations for Estimating Landslide-Triggering Factors Using Soil Characteristics

Kyeong-Su Kim ¹, Man-Il Kim ^{2,*} , Moon-Se Lee ³ and Eui-Soon Hwang ⁴

¹ Geologic Environment Division, Korea Institute of Geoscience and Mineral Resources, 124 Gwahak-ro, Yuseong-gu, Daejeon 34132, Korea; kks@kigam.re.kr

² Forest Engineering Research Institute, National Forestry Cooperative Federation, 1800 Dongseo-daero Daedeok-gu, Daejeon 34417, Korea

³ Institute of Slope Disaster Prevention, Association of Slope Disaster Prevention, 58 Namhyeon-gil, Gwanak-gu, Seoul 08804, Korea; landslides@daum.net

⁴ Korea Specialty Contractors Association, 15 Boramae-ro 5-gil, Dongjak-gu, Seoul 07071, Korea; euisoon1@naver.com

* Correspondence: mikim916@paran.com; Tel.: +82-42-341-1026

Received: 3 April 2020; Accepted: 19 May 2020; Published: 21 May 2020



Abstract: Landslides, which often occur on natural slopes of mountainous areas and artificial slopes around urban areas during summer in South Korea, are mostly caused by localized heavy rainfalls and typhoons. A survey was conducted, and the characteristics of landslide occurrences in different geological conditions—in this case, granite soils in Sangju area and gneiss soils in Yangu area—were analyzed. Soil characteristics in the landslide and non-landslide areas and the surroundings of each geological condition were also evaluated. Triggering factors, namely permeability coefficients (k), shear strength with cohesion (c), and internal friction angle (φ) of soils that are closely linked to landslides around weathered soil layers were extracted based on the examined characteristics and a statistics method. The study used regression analysis to formulate equations to estimate the permeability coefficients and shear strength. Ultimately, the permeability coefficients showed significant results in terms of void ratio (e), the effective size of grains (D_{10}), and uniformity coefficient (c_u), while shear strength correlated with the proportion of fine-grained soil (*Fines*), uniformity coefficient (c_u), degree of saturation (S), dry weight density (r_d), and void ratio (e).

Keywords: landslide-triggering factors; weathered soil; permeability coefficient; shear strength; regression equation

1. Introduction

In mountainous areas, active site renovations are frequently performed to expand human living spaces by building facilities in South Korea. This leads to the formation of vast fill and cut slopes in the developed sites. Every year, localized heavy rainfall causes frequent, extensive slope disasters, such as slope failures and landslides. Areas that have undergone mountainous development commonly experience these disasters, which may also lead to debris flow when materials that have been swept away are washed down to a nearby stream. Mountainous areas in South Korea damaged from landslides have sharply increased by two-and-a-half times, destroying 290 ha in the 1970s to 713 ha in the 2000s [1]. Such a significant escalation was accompanied by an increasing cost of landslide restoration.

There have been many notable landslide disasters in the developed mountainous areas of South Korea. The Umyeonsan landslides in Seoul on 27 July 2011, caused by heavy rains higher than the 100-year return period of rainfall at up to 94 mm/h, caused 18 deaths and buried roads and apartments

in the lower areas. On the same day, debris from landslides swept away houses and accommodations in Chuncheon in Gangwon Province, causing 13 deaths and 25 injuries [2,3]. These two cases were similar in terms of the localized heavy rainfall during the summer season around the cut slopes, which were formed after the natural slopes have been cut [4].

Rainfall is considered as one of the major causes of landslides. The penetration of stormwater through the soil layers increases the weights per unit volume of soil particles; thus slope stability rapidly decreases with the shear stress reduction of the soil [5–15]. Other direct and indirect causes of landslides include topography, geological features, and vegetation [16–19].

In most cases of natural slopes, weathering soil layers located at the upper part of bedrocks are formed with the erosion of parent rocks, and their physical and engineering characteristics are determined by weathering intensity and geological conditions [20,21]. Moreover, weathering soil layers have different properties depending on the mineral components of the bedrocks where they are created. In particular, the different geological types of rocks in slopes affect the factors that may cause landslides, such as weathering, shearing, cutting of bedrocks, directional nature of discontinuity surface, and water permeability [22–25].

The slip surface of landslides is commonly found around the boundary between the bedrock and the weathering soil layers. Hence, the physical characteristics of soil in these layers are closely linked with the occurrence of disasters [26,27]. More importantly, heavy rainfall influences the change in permeability and shear stress of weathering layers. It triggers the penetration of stormwater through the layers and decreases the shear stress of soils, increasing the possibility of disasters along the slope [28–32]. Therefore, the soil's permeability coefficient and shear strength are important variables for the direct assessment of slope stability considering infiltration of rainwater into the ground [33–36].

The study suggests that influential factors are related to slope disasters, which were identified by comparing the soil material properties of landslide and non-landslide areas to select the components that play significant roles during slope disasters and to derive a statistical formula for calculation. Moreover, the study considered the physical characteristics of the soil layers found in slopes and selected gneiss and granite for examination. An analysis was also conducted to understand rainfall events, topography, geological features, and the characteristics of landslides in the areas. Ultimately, the study suggested a statistical formula for the evaluation of landslide-triggering factors out of the properties that were closely linked to landslides for each soil type.

2. Methodology

2.1. Soil Properties of Landslide Areas

The study statistically analyzed the soil properties of landslides that occurred in slopes composed of gneiss and granite soils. A correlation analysis was conducted to discover whether there are distinctions in the soil properties of landslide areas based on their geological weathering conditions. In addition, regression equations for permeability coefficient and shear strength, which are the main variables linked to landslide-triggering factors based on soil properties, were suggested.

The selected sites for this study were areas with different geological features that have experienced multiple landslides caused by localized heavy rainfall within the same period. As such, the study focused on cities in South Korea, namely Yangju, Gyeonggi-do, and Sangju, Gyeongsangbuk-do, whose primary soil types were gneiss and granite, and 76 landslides in 1998 and 99 landslides in 1998 have occurred, respectively.

Figure 1 shows the field survey of landslides in Yangju, Gyeonggi-do, a study area, and shows that soil samples are collected using a cylindrical stainless ring sampler around the landslides. Soil samples were collected from their landslide and non-landslide areas, and soil characteristics were analyzed for each.

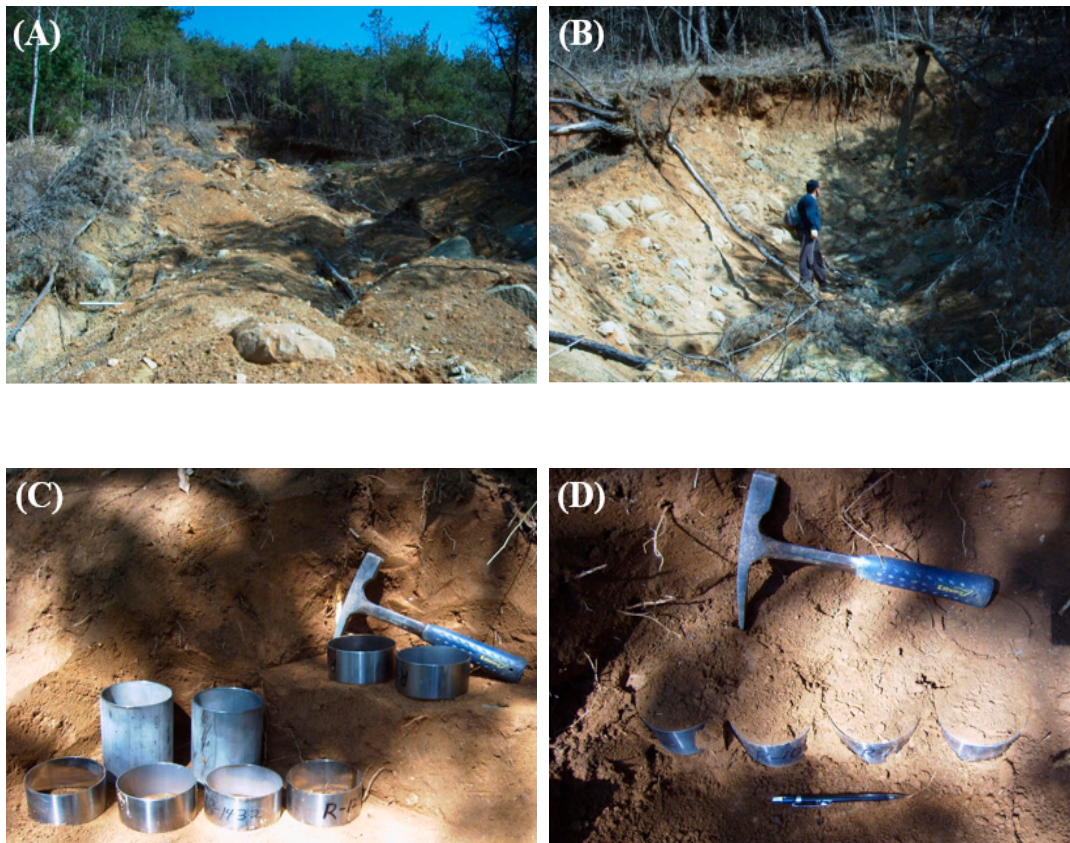


Figure 1. Measurement of the landslide scales through field surveys of landslides in the study area and sampling soil samples using a cylindrical stainless ring sampler (diameter 10 cm, height 6–15 cm) at a depth of about 40–60 cm of the ground after removing the topsoil; (A) View of landslide in Yangju, Gyeonggi-do. (B) Measurement of landslide length (using tapeline). (C) Before sampling soil samples using a cylindrical stainless ring sampler. (D) After inserting the cylindrical ring sampler by hitting it with a hammer, sampling the soil sample.

In the selected sites, soil sampling and analysis were performed as follows. Disturbed and non-disturbed samples were separately collected by removing the topsoil at a depth of 40–60 cm. For non-disturbed samples, a stainless cylindrical ring sampler that was 10 cm in diameter and 6–15 cm in height was produced. Meanwhile, two zipper bags with a volume of 250 g were used to obtain disturbed samples at the same area where the non-disturbed samples were collected. Then, all samples collected were sealed to maintain the field conditions as much as possible and were delivered to the laboratory for indoor testing. The indoor soil tests, which followed the Korean Industrial Standards (KIS), included a grain-size analysis [37], test for the water content of soils [38], specific gravity test [39], density test [40], and permeability test [41]. Finally, the permeability coefficient, micro-granule soil content, water content by weight, dry unit weight, and void ratio were calculated based on the test results.

2.2. Estimation of Landslide-Triggering Factors Using Soil Properties

The permeability test in landslide studies was conducted to find the permeability coefficient through constant and variable head permeability tests on the unsaturated sample. The shear test, on the other hand, determined the shear characteristics of the slope by obtaining the cohesive force and internal friction angle through a triaxial test, ring shear test, and direct shear test. Furthermore, slope stability decreased sharply when the soil layer was almost saturated with water content and reached the maximum shear stress, which eventually led to a failure.

Reproducing the permeability coefficient and shear strength characteristics of the soil slope corresponding to the landslide occurrence conditions and different geological materials was difficult. Therefore, studies relied on the characteristics of permeability coefficient at saturation and shear strength obtained at extremely limited shear rates. However, the greatest advantage of the direct shear test was that the shear strength properties of the soil were identified relatively more accurate, quicker, and easier compared to other test methods.

As such, the test methods for measuring the permeability coefficient and shear strength were more complicated than the test for the basic physical properties of soil and required expert skills. However, permeability coefficients and shear strength constants of various points were required to understand the soil characteristics and identify the failure mechanism in the landslide areas [42,43]. Thus, a considerable amount of time and costs were necessary to obtain the results.

The permeability of soil was affected by grain size distribution typically described by the equivalent particle diameters D_{10} and D_{60} , which corresponds to 10% and 60% passing by weight, respectively. Here, the descriptive parameter of grain size distribution is the coefficient of uniformity (c_u), which is defined as the ratio of $D_{60}-D_{10}$. A higher value of c_u is indicative of a well-graded soil that has a lower permeability coefficient compared to uniformly graded soil as the smaller grain fills the voids between larger grains, resulting in less interconnectivity.

Several correlations were developed to evaluate the permeability coefficient using the grain size [44–48]. The most commonly used correlation proposed by Hazen [49] is presented below:

$$k \text{ (m/s)} = C D_{10}^2 \quad (1)$$

where C is a constant that varies between 0.1 and 100 [50]. However, the typical values of C range between 0.4 and 1.2 and are typically taken as 1 [51]. In addition, the permeability coefficient can be raised by increasing the void ratios as particle shape and void arrangements also affect this variable. Hence, soils with angular particles exhibit a lower permeability coefficient compared to more rounded particles.

Particle size is one of the most important properties that play dominant roles in the stress, strain, and strength response of the soil. In particular, changes in particle size indicate changes in porosity, particle effective contact area, and the load distribution mechanism of soil particle contact as well [52].

Kolbuszewski and Frederick [53] and Chattopadhyya and Saha [54] used particle materials for evaluating the effects of particle size and confirmed that maximum porosity lowers while compressibility rises when the particle size increases.

According to studies on numerical analysis, the distribution of particle size influenced the stress-strain behavior of soil mass changes, which resulted in a decrease in the angles of internal friction and an increase in volumetric strain [55,56].

If the permeability coefficient and shear strength can be estimated roughly using the soil test results, which were relatively simple and inexpensive, then the soil characteristics in landslide areas can be identified more quickly and easily. The change of dependent variables (permeability coefficient and shear strength) from the change of independent variables (soil properties) can be estimated by analyzing the correlation between permeability coefficient and shear strength constant in slopes where landslides took place.

2.3. Statistical Analysis Using SPSS

To estimate landslide triggering factors through soil test results, correlation and regression analysis were used as statistical analysis using SPSS [57] in this study. Correlation analysis is widely used as a traditional statistical method to analyze the correlations between independent and dependent variables [58]. It evaluates the presence or absence of a linear relationship between two variables. Therefore, the main purpose of correlation analysis is to verify if a relationship exists, not to find out what functional relations there are between the variables. However, there are often cases where one

wants to predict the value of a variable from other variables. In this case, regression analysis can be used, which is a statistical analysis method that estimates a mathematical model from the data or makes a correlation through statistical inference.

Correlation analysis predicts the change of scale and direction of other variables as one variable increase or decrease. As such, the correlation is determined by how much of the variance (variate) of one variable changes as other variables' variance change, which is the covariance (covariate). Another important factor in correlation analysis is the correlation coefficient, which is an index that summarizes the degree and direction of a relationship between variables with a single numerical value, an absolute value between 0 and 1. The closer the correlation coefficient is to 0, the lower the correlation, and the closer to the absolute value 1, the higher the correlation.

Regression analysis is a method used to predict values, which is often a way to understand the extent and direction of one or more variables affecting another variable and analyze how the dependent variable (Y) changes as the independent variables (X) change. Once the values of the slope B and the Y-intercept A are determined, and the regression equation is obtained, it can predict the value of Y with the value of X.

Here, RMSE is the square root of the mean of the squared error between the value predicted from an estimate or model equation and the value observed in a real soil environment. It is a method to check the difference between the predicted value and the real soil experiment and observation results. Furthermore, the correlation and suitability of regression model results and direct experiment results were evaluated.

3. Results

3.1. Rainfall Events

Figure 2 shows rainfall events at the time when landslides occurred intensively in the study area. The Yangju area in Gyeonggi-do analyzed rainfall data from Geumcheon, Uijeongbu, and Goyang weather stations close to the area where the landslide occurred. From 4 August to 7 August 1998, a cumulative rainfall of up to 588.5 mm fell. During the rainfall period, on 7 August, many landslides occurred in Yangju area due to 111.5 mm/h of intensive rainfall. In Sangju, Gyeongsangbuk-do, rainfall data from Boeun, Hwaseo, and Anggye weather stations were analyzed. From 10 August to 12 August 1998, a cumulative rainfall of 522 mm occurred. The landslide occurred on 12 August due to a rainfall of 95 mm/h. It was analyzed that the rainfall pattern when the landslide occurred intensively in the study area was within 3–4 days of rainfall duration and the cumulative rainfall was more than 500 mm.

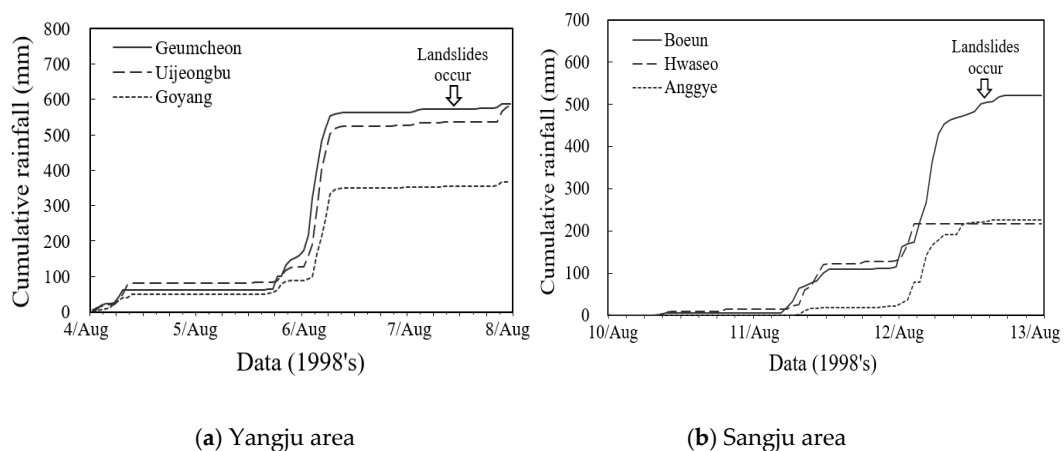


Figure 2. Changes in cumulative rainfall observed at meteorological stations located around the study area based on when the landslide occurred.

3.2. Landslide Pattern

Factors such as terrain complexity and geometry are closely related to the occurrence and spatial distribution of various types of landslides [59–61]. Key direct factors of the landslide are topography, geological characteristics, and rainfall. The study areas located in South Korea are composed of two different major geological types. One is Yangju, Gyeonggi-do, a gneiss region, while the other is in Sangju, Gyeongsangbuk-do, a granite region. Most of the landslides in these areas occurred during the heavy rains in early August, affecting 175 sites, including 76 for gneiss and 99 for granite.

Figure 3 shows the locations of landslides in the areas of study as well as their geological distribution. In Yangju, Gyeonggi-do, the destructive patterns of landslides in gneiss regions started with translational slides that changed into flows as the landslide materials moved to lower slopes. Thus, it was found that a translational type plane destruction occurred on a relatively flat slope, and the destroyed materials moved downward, mixing with surrounding materials, and transformed into a debris flow going further down the V-shaped valley. Moreover, a shallow solum that consisted of residual and colluvial soils was found to have collapsed along with the interface of the bedrock. In Sangju, Gyeongsangbuk-do, granite was widely distributed, while sedimentary rocks were partly distributed. Landslides occurred widely in the totality of the landscape but were more frequent in granite areas. Furthermore, landslides in this area were mostly found to be of translational-type flow, most of which were relatively shallow at depths of less than 1 m, while the upper soil layers, which consist of residual and colluvial soils, collapsed along the boundary of the bedrock. It was also shown that landslide materials moved to the bottom of the slope and became a flow. Overall, landslide patterns in the granite region were found to be similar to gneiss areas.

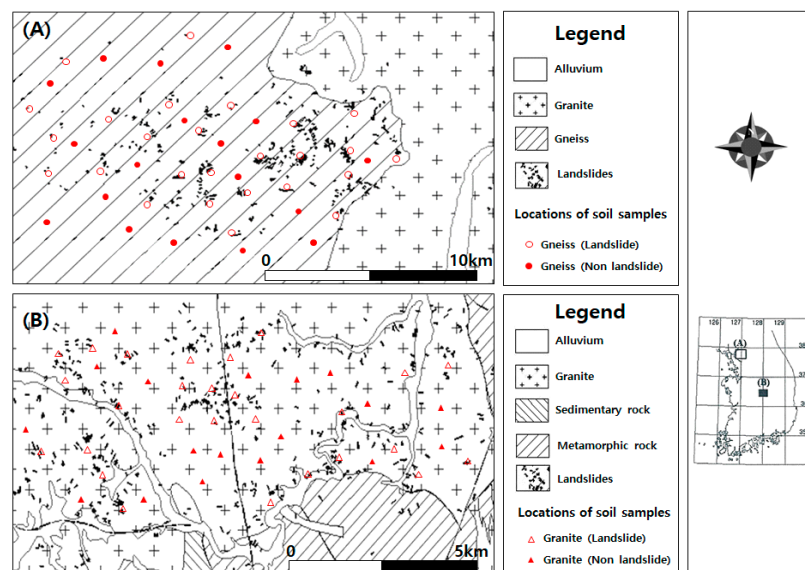


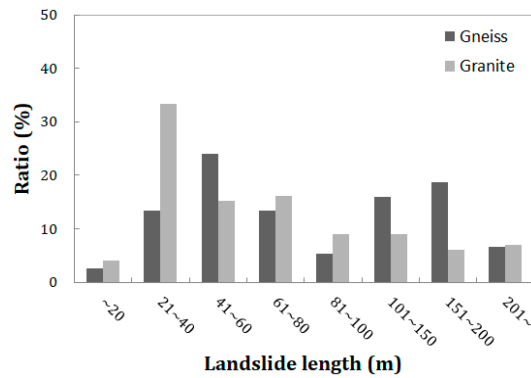
Figure 3. Geological status map including soil sampling points for landslides and non-landslides regions in the areas of study. (A) Landslides in Yangju, Gyeonggi-do. (B) Landslides in Sangju, Gyeongsangbuk-do.

3.3. Landslide Scales

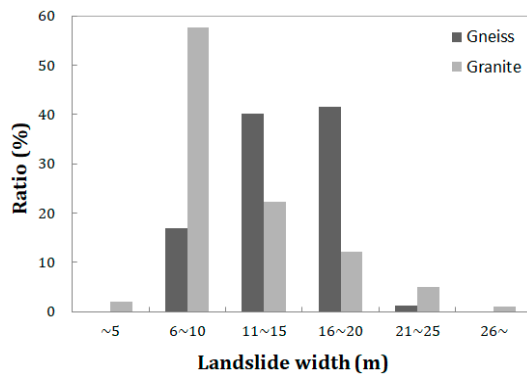
Landslide patterns in the areas of study mostly changed from translational-type to flow-type. Translational-type landslides were largest in the granite area at about 98% compared to 75% in the gneiss area. In particular, most of the translational-type landslides in the granite area showed a shallow collapse that formed along the interface of the bedrock. Subsequently, the collapsed soil material developed into a flow.

Figure 4 shows the length, width, and depth of landslides depending on the geology of the study area. The scale of landslides in the gneiss area ranged from 20 m to 290 m based on the length. On a 20 m criteria, 41–60 m accounted for the highest occupancy rate of about 24% with 18 sites recorded among

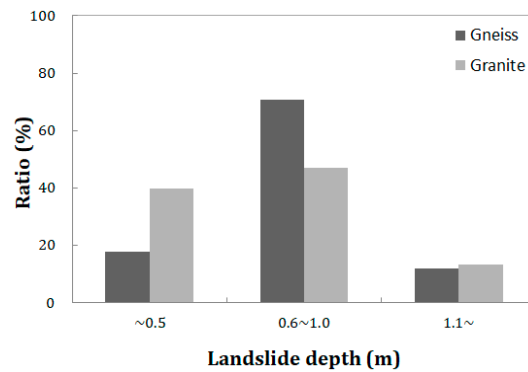
77 outbreaks, followed by 61–80 m and 21–40 m, which occupied about 13%, in 10 sites, respectively. On the other hand, landslides of over 100 m in length accounted for 31 out of 77 sites, which was about 42%, revealing that several long-length landslides occurred.



(a) Landslide length



(b) Landslide width



(c) Landslide depth

Figure 4. Analysis of landslide occurrence patterns of different geological features in the study area.

Moreover, the length of landslides in the gneiss region ranged from 8 m to 22 m, with 16–20 m and 11–15 m accounting for about 42% and about 40%, respectively, taking up the most impact. In contrast, about 58% of landslides in the granite region came within the 6–10 m length interval, on account of the gentle V-shaped water sump type topography of the landslide site.

More than about 88% of landslides in these areas were found to have occurred within a depth of 1 m as landslides often occur in areas with low slopes, and outcrops are well developed on slopes at higher elevations, resulting in relatively low rates of landslides. In addition, the depth of landslides was considered shallow because destruction occurred at the boundary between the shallow top layer, which consists of residual and colluvial soils, and the bedrock.

3.4. Soil Properties of Landslide and Non-Landslide Areas

Soil layers in landslide areas are known to have finer soil particles and smaller liquid limits than in non-landslide areas [62,63]. Soil particle size distribution is also an important factor in landslides. In flow-type landslides, soil particle size analysis is performed. If there are 20–80% particles of 2 mm or more in diameter, they are classified as a debris flow. On the other hand, it is considered soil flow if it contains 80% or more of particles less than 2 mm in diameter [11].

Figure 5 shows the particle size test results for soil samples in the different geological features of the areas of study, categorized into the landslide and non-landslide areas in the soil particle size distribution curve. In the gneiss region, the soil particle size distribution curve is generally inclined

moderately, and coarse and fine-grained soil is moderately mixed. The uniformity coefficient ranges from 5 to 40; while the curvature coefficient, from 1 to 3, satisfying the qualifications for well-graded soil gradations. In addition, the soil particle size in landslide areas was found to be distributed more evenly, while particle size in non-landslide areas has similar distribution specifications.

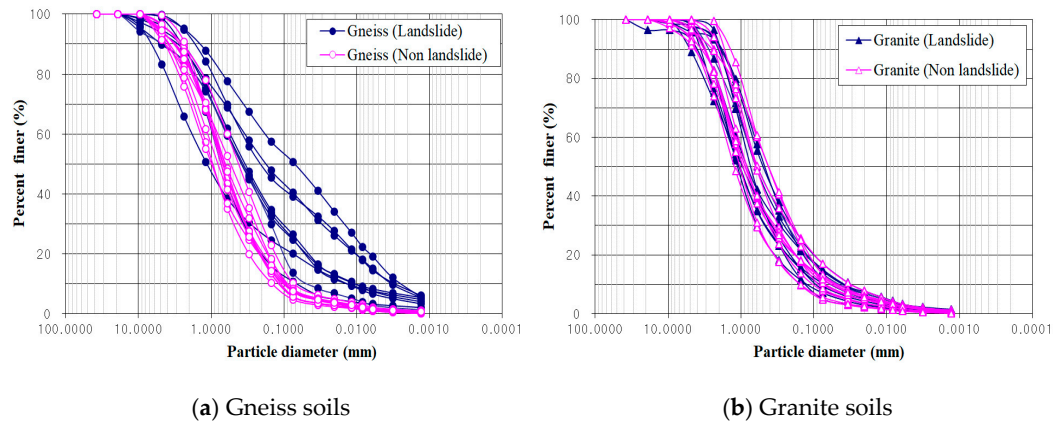


Figure 5. Soil particle size distribution curves for soil samples collected from landslides and non-landslide areas in gneiss and granite regions.

In the granite region, the soil particle size distribution curve showed a moderate slope, and the soils were more thoroughly mixed. Moreover, the uniformity coefficient ranges from 2 to 33; while the curvature coefficient, from 1 to 3, showing that the soil is indeed well-graded. In addition, the granite area showed the same particle size distribution patterns in both landslide and non-landslide areas.

Table 1 shows the constants for the characteristics of soil layers in the landslide areas of the gneiss and granite regions. The liquid limit showed a similar tendency, whereas the plastic limit of the soil surface was found to be higher in the gneiss region. Moreover, the plastic limit is a property that is directly related to the content of clay particles in the particle size distribution of the soil layer, which is consistent with the result that the gneiss region shows a higher content of fine-grained soil than the granite region.

Table 1. Soil characteristics in landslide occurrence areas.

Geology	Density, g/cm ³		Water Content, %		Liquid Limit, %		Plastic Limit, %	
	Range	Average	Range	Average	Range	Average	Range	Average
Gneiss	2.6–2.76	2.69	8.72–33.47	17.38	20.15–37.55	29.66	14.74–26.32	19.84
Granite	2.52–2.72	2.62	9.49–31.84	16.23	23.97–37.15	30.10	13.77–27.00	18.97
Geology	Void Ratio		Porosity, %		Dry Unit Weight, kN/m ³			
	Range	Average	Range	Average	Range	Average		
Gneiss	0.75–1.57	1.13	42.86–61.09	52.57	10.3–15.3	12.8		
Granite	0.76–1.29	1.03	43.18–56.33	50.49	11.5–14.7	13.0		
Geology	Permeability Coefficient, cm/s		Cohesion, kN/m ²		Internal Friction Angle, °			
	Range	Average	Range	Average	Range	Average		
Gneiss	1.33×10^{-5} – 2.17×10^{-4}	5.43×10^{-5}	1.6–29.6	8.8	18–38	33		
Granite	1.66×10^{-6} – 5.16×10^{-4}	6.00×10^{-5}	0.8–13.3	5.3	30–39	34		

Soils in the granite region had the highest permeability coefficient between the two regions. Meanwhile, this phenomenon may have been affected by other soil characteristics, such as particle size distribution, roughness, and structure, and geological properties, such as weathering or sedimentation environment.

3.5. Derivation of Regression Equations for Evaluating Landslide-Triggering Factors

3.5.1. Regression Equations of Permeability Coefficient

To select soil properties significant to the permeability coefficient, the study examined 16 properties for each sample obtained from the test results through the Pearson correlation analysis. As shown in Table 2, the Pearson correlation coefficient (r) and significance (F) can explain the correlation quantitatively. According to the Pearson correlation coefficient, the larger the number is and the closer its significance is to 0, the higher the correlation, regardless of whether the correlation is negative or positive. Furthermore, a negative correlation coefficient shows an inversely proportional relation, while a positive coefficient shows the opposite.

Table 2. Correlation coefficient and significance results between the permeability coefficient and characteristics of the soil through correlation analysis.

Soil Variable	Correlation	Permeability Coefficient, cm/s		Soil Variable	Correlation	Permeability Coefficient, cm/s	
		Gneiss	Granite			Gneiss	Granite
Density	r	0.293	0.118	Liquid limit, %	r	-0.167	0.373
	F	0.063	0.544		F	0.310	0.046
Water Content, %	r	0.045	-0.003	Plastic limit, %	r	-0.065	0.161
	F	0.781	0.987		F	0.694	0.404
Void Ratio	r	0.353	0.551	Gravel, %	r	0.100	0.067
	F	0.024	0.002		F	0.535	0.729
Porosity, %	r	0.238	0.213	Sand, %	r	0.139	0.124
	F	0.134	0.266		F	0.387	0.523
Degree of Saturation, %	r	-0.162	-0.229	Fine, %	r	-0.189	-0.315
	F	0.311	0.231		F	0.236	0.097
Wet unit Weight, kN/m ³	r	-0.294	-0.533	Effective grain size, D ₁₀ , cm	r	0.670	0.836
	F	0.062	0.003		F	0.000	0.000
Saturation Unit Weight, kN/m ³	r	-0.270	-0.413	Coefficient of uniformity, c_u	r	-0.627	-0.591
	F	0.088	0.026		F	0.000	0.001
Dry Unit weight, kN/m ³	r	-0.298	-0.504	Coefficient of curvature, c_g	r	0.060	-0.470
	F	0.058	0.005		F	0.711	0.010

Remarks: r is Pearson correlation coefficient, and F is significance.

As presented in Table 3, the soil properties with high significance for the permeability coefficient showed a high correlation with three soil properties, namely effective diameter, uniformity coefficient, and void ratio. Therefore, these properties were selected as independent variables for the regression analysis.

Table 3. Statistical results of permeability coefficient by the regression analysis of soils by different geological feature.

Geology	Soil Variable	Unstandardized Coefficients		Standardized Coefficients	t-value	Significance Probability, P
		B	Standard Error	Beta		
Gneiss	(Constant)	-1.893×10^{-2}	0.004		-5.004	0.000
	Effective grain size, D_{10}	1.076	0.161	0.774	6.683	0.000
	Coefficient of uniformity, c_u	-1.629×10^{-4}	0.000	-0.151	-1.350	0.185
	Void ration, e	1.488×10^{-2}	0.002	0.655	9.415	0.000
Granite	(Constant)	-9.907×10^{-3}	0.001		-7.831	0.000
	Effective grain size, D_{10}	8.281×10^{-3}	0.001	0.474	9.177	0.000
	Coefficient of uniformity, c_u	0.639	0.047	0.772	13.702	0.000
	Void ration, e	-2.766×10^{-5}	0.000	-0.058	-0.973	0.340

Using a two-step process in selecting the soil properties related to the permeability coefficient from the correlation coefficients determined through correlation and regression analysis, more accurate correlations were found, and the contribution of each soil property concerning the permeability coefficient is represented numerically as a regression equation.

Then, a simple regression analysis was performed by calculating the permeability coefficients in the permeability test using the effective diameter, uniformity coefficient, and the void ratio to derive the statistics-based equations of soil.

According to the results of regression analysis for the gneiss and granite regions, variance analysis, which is a measure of the accuracy of an equation, had a significant probability of $P = 0.000$, and the R-square representing explanatory power was about 83% in gneiss soil and about 93% in granite soil. This means that the regression equation was suitable. With this, the regression equations for estimating permeability coefficient in different geological conditions can be summarized as follows, using the unstandardized coefficient of regression equation results:

$$k_{gn} = (1.488 \times 10^{-02} \times e) + (1.076 \times D_{10}) + (-1.629 \times 10^{-04} \times c_u) - (1.893 \times 10^{-02}) \tag{2}$$

$$k_{gr} = (8.281 \times 10^{-03} \times e) + (0.639 \times D_{10}) + (-2.766 \times 10^{-05} \times c_u) - (9.907 \times 10^{-03}) \tag{3}$$

where k_{gn} is the permeability coefficient of gneiss soil, k_{gr} is the permeability coefficient of granite soil, D_{10} is the effective diameter, e is the void ratio, and c_u is uniformity coefficient, respectively.

3.5.2. Regression Equations of Shear Strength

To estimate the shear strength of soil in various geological features through the regression equation, the researchers used correlation analysis using various soil tests and analytical data on samples collected in the study sites similar to the estimation of the permeability coefficient. Pearson correlation analysis was conducted on the soil variables of 16 properties to select properties that are significant for shear strength with cohesion and internal friction angle. Pearson’s correlation coefficient and significance were obtained for cohesion and internal friction angle of soil, as shown in Table 4.

Table 4. Correlation coefficient and significance between cohesion and internal friction angle and soil characteristics.

Soil Variable	Correlation	Cohesion, kN/m ²		Internal Friction Angle, °	
		Gneiss	Granite	Gneiss	Granite
Density	<i>r</i>	0.634	0.297	0.635	0.219
	<i>F</i>	0.036	0.231	0.036	0.254
Water Content, %	<i>r</i>	−0.409	−0.642	−0.403	−0.351
	<i>F</i>	0.211	0.004	0.219	0.062
Void Ratio	<i>r</i>	−0.272	−0.093	−0.935	−0.808
	<i>F</i>	0.418	0.713	0.000	0.000
Porosity, %	<i>r</i>	0.146	0.546	−0.337	−0.287
	<i>F</i>	0.667	0.019	0.311	0.132
Degree of Saturation, %	<i>r</i>	−0.234	−0.687	0.112	−0.113
	<i>F</i>	0.489	0.002	0.743	0.559
Wet Unit Weight, kN/m ³	<i>r</i>	0.097	−0.294	0.826	0.679
	<i>F</i>	0.777	0.234	0.002	0.000
Saturation Unit Weight, kN/m ³	<i>r</i>	0.318	0.178	0.960	0.816
	<i>F</i>	0.341	0.481	0.000	0.000
Dry Unit Weight, kN/m ³	<i>r</i>	0.071	0.136	0.925	0.844
	<i>F</i>	0.837	0.590	0.000	0.000
Liquid Limit	<i>r</i>	−0.270	0.073	−0.502	−0.258
	<i>F</i>	0.423	0.775	0.115	0.177
Plastic Limit	<i>r</i>	−0.151	0.309	−0.475	0.247
	<i>F</i>	0.658	0.213	0.139	0.196
Gravel, %	<i>r</i>	0.215	0.419	0.032	−0.040
	<i>F</i>	0.525	0.084	0.927	0.835
Sand, %	<i>r</i>	0.534	0.125	0.198	0.252
	<i>F</i>	0.091	0.621	0.559	0.188
Fine, %	<i>r</i>	−0.947	−0.928	−0.219	−0.345
	<i>F</i>	0.000	0.000	0.518	0.067
Effective Grain Size, D ₁₀ , cm	<i>r</i>	0.480	0.606	0.599	−0.043
	<i>F</i>	0.135	0.008	0.052	0.826
Coefficient of Uniformity, <i>c_u</i>	<i>r</i>	−0.746	−0.417	−0.374	−0.008
	<i>F</i>	0.008	0.086	0.257	0.966
Coefficient of Curvature, <i>c_g</i>	<i>r</i>	0.551	−0.403	0.147	0.197
	<i>F</i>	0.079	0.097	0.666	0.307

Remarks: *r* is Pearson correlation coefficient, and *F* is significance.

For the gneiss region, the soil properties with a high significance level for cohesion were fine grain content and uniformity coefficient. Therefore, the two were selected as independent variables for regression analysis. Meanwhile, the soil properties that produced high significance for internal friction angle were void ratio, saturation unit weight, and dry unit weight. As the saturation unit weight and dry unit weight are proportional to each other, only void ratio and dry unit weight were selected as independent variables to be applied to the regression analysis to simplify the equation.

The properties with a high significance level to cohesion in granite soils were found to be as follows: fine-grain soil content, saturation, effective diameter, and uniformity coefficient. Among these properties, the significance of the equality coefficient was 0.086, which is greater than the significant level of 0.05 from a statistical point of view, leading to the exclusion of the equality coefficient from the equation, and adding the degree of saturation and effective diameter instead. Finally, only fine-grained

soil content and saturation degree were selected as independent variables for regression analysis to simplify the equations.

For the granite regions, soil properties with equally high significance levels for internal friction angle were the void ratio, dry unit weight, wet unit weight, and saturated unit weight. Hence, void ratio and dry unit weight were finalized as the independent variables for regression analysis to simplify the regression equation that is consistent with the gneiss model.

As shown in Table 5, a simple regression analysis of the soils by geological feature was used to derive the ground variables with high correlations between soil properties to make a regression equation for estimating the cohesion and internal friction angles of the gneiss and granite soils.

Table 5. Statistical results of shear strength with cohesion and internal friction angle using regression analysis of soils in different geological features.

Geology	Soil Variable	Unstandardized Coefficients		Standardized Coefficients	t-value	Significance Probability, P	
		B	Standard Error	Beta			
Gneiss	(Constant)	15.335	1.479		10.369	0.000	
	Cohesion, kN/m ²	Fine grain content, <i>Fines</i>	-0.712	0.130	-0.851	-5.457	0.001
		Coefficient of uniformity, <i>c_u</i>	-0.131	0.151	-0.135	-0.863	0.413
	Internal Friction Angle, °	(Constant)	6.018	10.509		0.573	0.583
		Void ratio, <i>e</i>	-12.594	2.566	-0.543	-4.909	0.001
		Dry unit weight, <i>r_d</i>	27.010	6.047	0.494	4.466	0.002
Granite	(Constant)	18.590	0.871		21.347	0.000	
	Cohesion, kN/m ²	Fine grain content, <i>Fines</i>	-0.698	0.072	-0.779	-9.701	0.000
		Degree of saturation, <i>S</i>	-7.441 × 10 ⁻²	0.020	-0.298	-3.709	0.002
	Internal Friction Angle, °	(Constant)	-9.685	27.740		-0.349	0.730
		Void ratio, <i>e</i>	-0.875	9.138	-0.033	-0.096	0.924
		Dry unit weight, <i>r_d</i>	33.640	14.381	0.813	2.339	0.027

According to the regression analysis, the variance analysis, which is a measure of the accuracy of the gneiss cohesion model, showed a very good probability of P = 0.000, and the R-square representing the explanatory power was about 88%. Moreover, the regression equation for internal friction angles was deemed suitable with the probability of P = 0.000, and an R-square of about 96%. Therefore, the final regression equations for the cohesion and internal friction angle of gneiss soil are shown as Equations (4) and (5):

$$c'_{gn} = (-0.712 \times Fines) + (-0.131 \times c_u) + 15.335 \tag{4}$$

$$\phi'_{gn} = (27.01 \times r_d) + (-12.594 \times e) + 6.018 \tag{5}$$

where c'_{gn} is the cohesion of gneiss soil, ϕ'_{gn} is the internal friction angle of gneiss soil, *Fines* is fine-grained soil content, c_u is the uniformity coefficient, r_d is dry unit weight, and *e* is the void ratio, respectively.

Meanwhile, the results of the regression analysis of the granite cohesion model showed a very good probability of $P = 0.000$ and an R-square of about 92%. For the internal friction angle, the probability of variance analysis showed $P = 0.000$, and the R-square about 70%. Finally, the regression equations for estimating the cohesion of granite soils is shown in Equation (6). On the other hand, the internal friction angle estimation equation of the granite soil is shown in Equation (7):

$$c'_{gr} = (-0.689 \times Fines) + (-0.0744 \times S) + 18.590 \tag{6}$$

$$\varphi'_{gr} = (33.640 \times r_d) + (-0.875 \times e) - 9.685 \tag{7}$$

where, c'_{gr} is the cohesion of granite soil, φ'_{gr} is the internal friction angle of granite soil, $Fines$ is fine-grained soil content, S is the degree of saturation, r_d is dry unit weight, and e is the void ratio, respectively.

4. Discussion

4.1. Validation of Permeability Coefficients

To validate the regression equations for estimating the permeability coefficient in the gneiss region, this study analyzed the results of the estimation equation and the permeability test on 26 soil samples from landslide areas and 18 samples from non-landslide areas. In addition, 27 sample soils from landslide areas and 18 sample soils from non-landslide areas were verified using the same method for the estimation equation for the granite soil.

Figure 6 shows the results of the permeability test and regression analysis by landslide occurrence. The relationships between the two permeability coefficients in the gneiss region were verified to have a significant R-square of about 87.1% in landslide soil layers and about 84.5% in non-landslide soil layers. In the granite region, landslide soil layers showed a highly significant R-square of about 96.6% and about 94.0% in non-landslide areas.

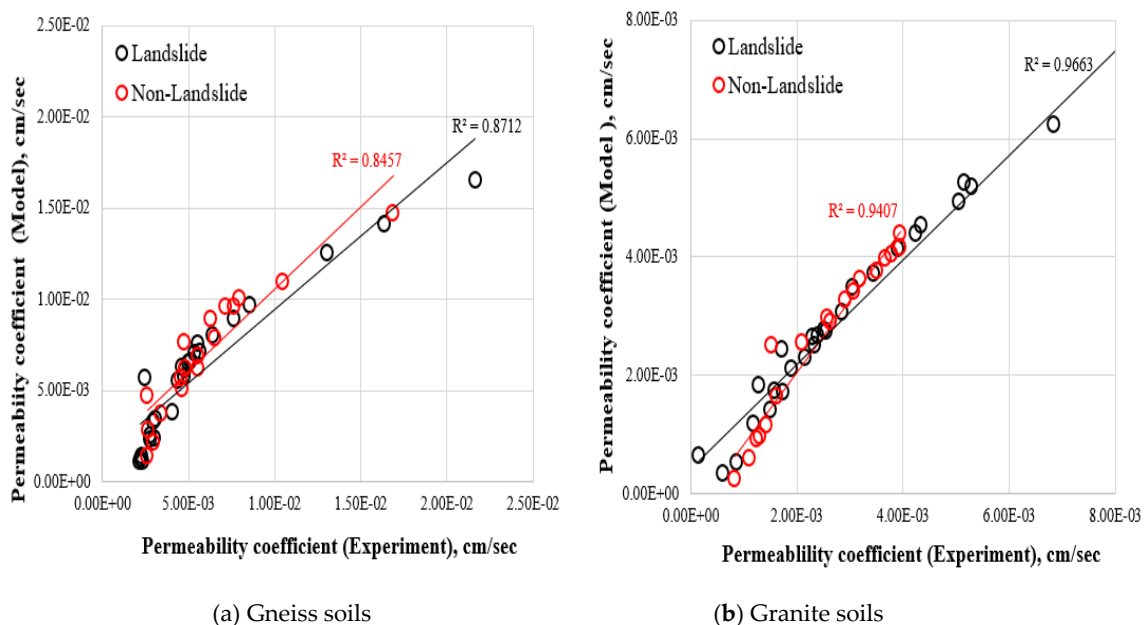


Figure 6. Comparison of permeability coefficient factor estimations for landslide and non-landslide soils in areas of study.

As a result of verifying the significance of the regression equation developed through RMSE as shown in Table 6, the root of mean square error of the permeability coefficient test results and the

regression analysis value was considered to be significant as they are within the tolerance range of 0.1 or less.

Table 6. Results of RMSE analysis of permeability coefficients in soils per geological feature.

Soil Variable	Type	Gneiss Soil		Granite Soil	
		MSE	RMSE	MSE	RMSE
Permeability coefficient, cm/s	Landslide	2.864×10^{-6}	1.692×10^{-3}	1.536×10^{-7}	3.919×10^{-4}
	Non-landslide	2.738×10^{-6}	1.654×10^{-3}	1.769×10^{-7}	4.206×10^{-4}

Remarks: MSE is mean squared error, and RMSE is root mean squared error.

4.2. Validation of Shear Strengths

To validate the regression equations for estimating shear strength with cohesion and internal friction angle for gneiss soil, this study analyzed the results of the regression equation and the soil tests on 11 sample soils from landslide areas and eight samples from non-landslide areas. Furthermore, 18 sample soils from landslide areas and 14 sample soils from non-landslide areas were verified using the same method for the regression equation for granite soil.

Figures 7 and 8 show the correlation between the test results and the estimation values of coherence and internal friction angle for landslide and non-landslide areas. Results from samples taken from landslide areas in the gneiss region showed high correlations of about 90.6% cohesion and about 96.3% internal friction angle, while results from non-landslide areas were about 81.3% for cohesion and about 97.3% for internal friction angle. In samples taken from landslide areas in the granite region, correlations of about 92.7% for cohesion and about 84.8% for internal friction angle have been verified. Results from non-landslide areas showed about 91.9% for cohesion and about 85.0% for internal friction angle.

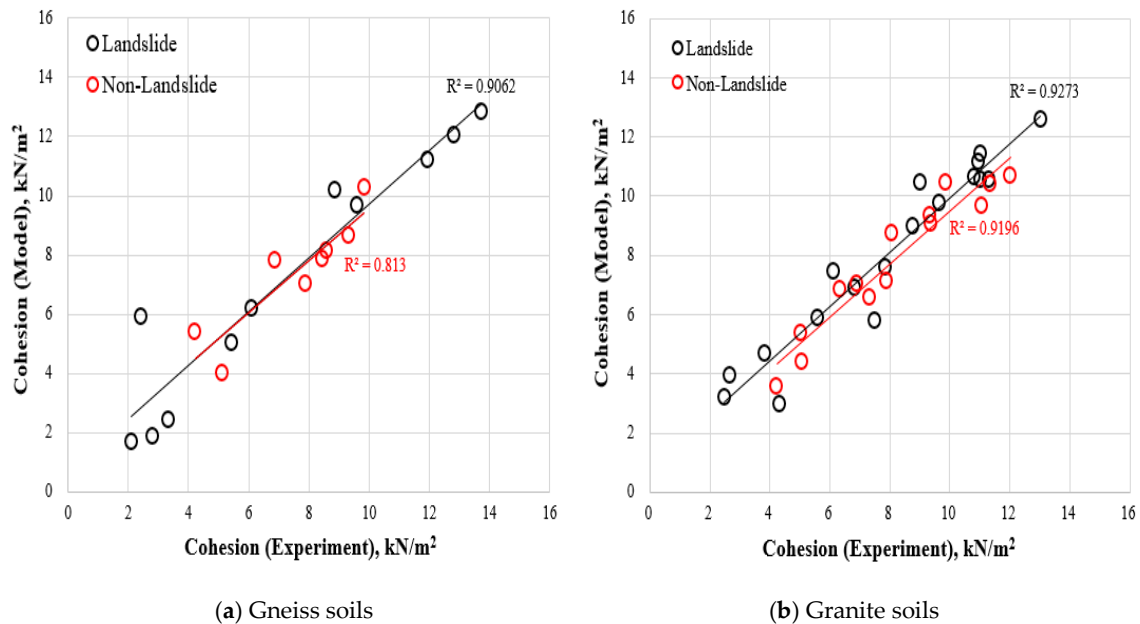


Figure 7. Comparison of cohesion factor estimations for landslide and non-landslide soils in areas of study.

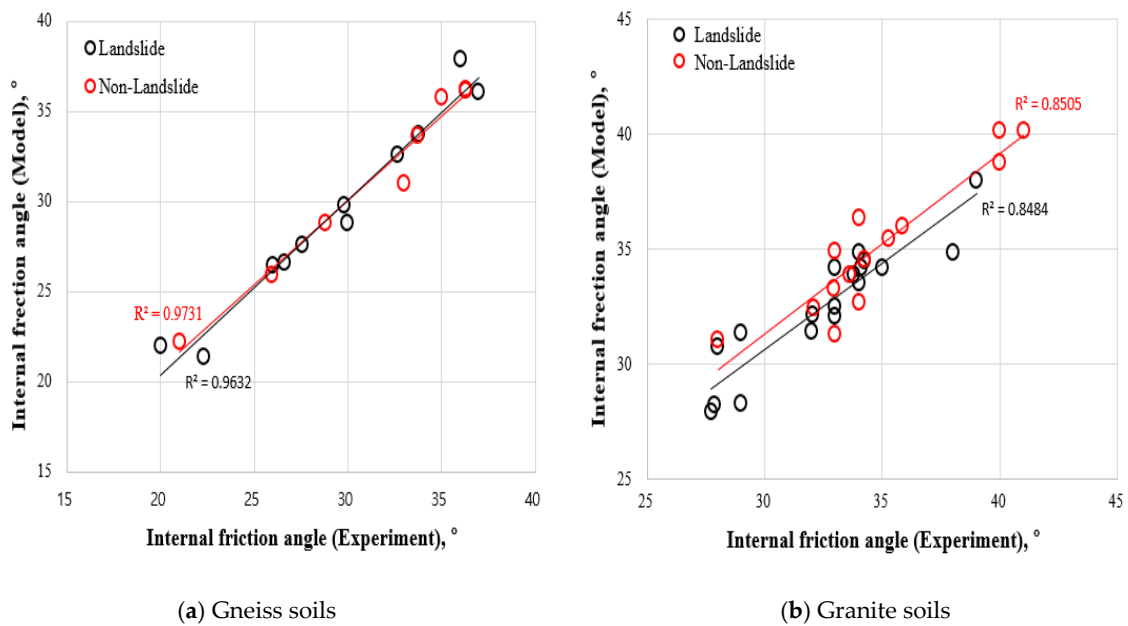


Figure 8. Comparison of internal friction angle factor estimations for landslide and non-landslide soils in areas of study.

As shown in Table 7, in the results of verifying the importance of the regression equation developed through RMSE, the root and regression analysis values of the mean square root of the shear test results were evaluated to be significant in the tolerance range of 0.1 or less.

Table 7. Results of RMSE analysis of cohesion and internal friction angle in soils per geological feature.

Soil variable	Type	Gneiss Soil		Granite Soil	
		MSE	RMSE	MSE	RMSE
Cohesion, kN/m ²	Landslide	1.643	1.282	0.722	0.850
	Non-landslide	0.692	0.831	0.559	0.748
Internal Friction Angle, °	Landslide	0.987	0.993	1.633	1.278
	Non-landslide	0.761	0.872	1.854	1.361

Remarks: MSE is mean squared error, and RMSE is root mean squared error.

5. Conclusions

This study investigated different characteristics of landslide occurrences in areas with gneiss and granite soils. In addition, regression equations for landslide-triggering factors using soil properties were developed to estimate the permeability coefficient and shear strength in relation to the cohesion and internal friction angle of different weathered soils that affect landslides.

The occurrence of landslides is directly affected by large porosity and minimal density of soil materials as soils in landslide areas have poor soil particle size distributions and loose ground conditions. Therefore, these types of soils are relatively more vulnerable to landslides under similar geological conditions.

When the correlations between the soil parameters of gneiss and granite regions were analyzed, the permeability coefficient was found to have a significant correlation with the void ratio, the effective diameter, and the uniformity coefficient, while shear strength had a significant correlation with fine grain content, uniformity coefficient, saturation, dry density, and void ratio.

As such, the regression equations were developed to easily calculate the permeability coefficient and shear strength (cohesion and internal friction angle), which were considered important in landslide

areas, using only the properties that had a significant correlation with the soils. These estimation results were then analyzed to gain a correlation to the actual test results of at least about 81%. The regression equations were deemed suitable for the study and were used to calculate the permeability coefficient and shear strength with cohesion and internal friction angle in unsaturated soils of natural slopes under certain geological conditions using simple soil properties.

The current study is limited to a statistical analysis to estimate landslide-triggering factors using soil properties for the study area comprising of granite and gneiss. Therefore, it is likely that these results may have limited implications beyond this particular study area. Future research is therefore needed to assess the wider application of this approach to other areas, and to also consider the inclusion of unsaturated characteristics for different soil types along with the physical relationships between the soil properties and landslide triggering mechanisms.

Author Contributions: Conceptualization, K.-S.K. and E.-S.H.; Data curation, K.-S.K. and M.-S.L.; methodology, M.-I.K. and M.-S.L.; writing—original draft preparation, K.-S.K. and M.-I.K.; writing—review and editing, K.-S.K., E.-S.H. and M.-I.K.; All authors have read and agreed to the published version of the manuscript.

Funding: This research was supported by the Korea Institute of Geoscience and Mineral Resources (KIGAM) Research Project (19-3413). Furthermore, the reanalysis of the research data and paperwork was supported by the Korea Agency for Infrastructure Technology Advancement under the Ministry of Land, Infrastructure, and Transport of the Korean government (Project Number: 20SCIP-C151408-02).

Conflicts of Interest: The authors declare no conflict of interest.

References

- Oh, S.; Lee, G.; Bae, W. Estimation of landslide risk based on infinity flow direction. *J. Korean Geo-Environ. Soc.* **2019**, *20*, 5–18. (In Korean with English Abstract)
- Seoul Metropolitan Government (SMG). The 1st final inspection report on causes and restoration works of the 2011 Umyeonsan landslides. In *Korean Geotechnical Society*; Seoul Metropolitan Government: Seoul, Korea, 2011; 262p.
- Lee, S.-G.; Winter, M.G. The effects of debris flow in the Republic of Korea and some issues for successful risk reduction. *Eng. Geol.* **2019**, *251*, 172–189. [[CrossRef](#)]
- Nam, D.H.; Kim, M.-I.; Kang, D.-H.; Kim, B.S. Debris flow damage assessment by considering debris flow direction and direction angle of structure in South Korea. *Water* **2019**, *11*, 328. [[CrossRef](#)]
- Mathewson, C.C.; Keaton, J.R.; Santi, P.M. Role of bedrock ground water in the initiation of debris flows and sustained post flow stream discharge. *Bull. Assoc. Eng. Geol.* **1990**, *27*, 73–83. [[CrossRef](#)]
- Sitar, N.; Anderson, S.A.; Johnson, K.A. Conditions leading to the initiation of rainfall-induced debris flows. In Proceedings of the Geotechnical Engineering Division Specialty Conference: Stability and Performance of Slopes and Embankments-II, ASCE, New York, NY, USA, June 29–July 1 1992; pp. 834–839.
- Montgomery, D.R.; Schmidt, K.M.; Greenberg, H.M.; Dietrich, W.E. Forest clearing and regional landsliding. *Geology* **2000**, *28*, 311–314. [[CrossRef](#)]
- Kim, J.-W.; Shin, H.-S. Slope stability assessment on a landslide risk area in Ulsan during rainfall. *J. Korean Geotech. Soc.* **2016**, *32*, 27–40. (In Korean with English Abstract) [[CrossRef](#)]
- Jeong, S.; Lee, K.; Kim, J.; Kim, Y. Analysis of rainfall-induced landslide on unsaturated soil slopes. *Sustainability* **2017**, *9*, 1280. [[CrossRef](#)]
- Ran, Q.; Hong, Y.; Li, W.; Gao, J. A modelling study of rainfall-induced shallow landslide mechanisms under different rainfall characteristics. *J. Hydrol.* **2018**, *563*, 790–801. [[CrossRef](#)]
- Varnes, D.J. *Slope Movement Types and Process*; Special Report; National Academy of Science: Washington, DC, USA, 1978; Volume 2, pp. 11–33.
- Brand, E.W. Some thoughts on rain-induced slope failures. In Proceedings of the 10th International Conference on Soil Mechanics Foundation Engineering, Stockholm, The Netherlands, 15–19 June 1981; pp. 373–376.
- Cho, S.E. Probabilistic stability analysis of rainfall-induced landslides considering spatial variability of permeability. *Eng. Geol.* **2014**, *171*, 11–20. [[CrossRef](#)]

14. Hong, H.; Chen, W.; Xu, C.; Youssef, A.M.; Pradha, B.; Bui, D.T. Rainfall-induced landslide susceptibility assessment at the Chongren area (China) using frequency ratio, certainty factor, and index of entropy. *Geocarto Int.* **2017**, *32*, 139–154. [[CrossRef](#)]
15. Tang, G.; Huang, J.; Sheng, D.; Sloan, S.W. Stability analysis of unsaturated soil slopes under random rainfall patterns. *Eng. Geol.* **2018**, *245*, 322–332. [[CrossRef](#)]
16. Olivier, M.; Bell, F.G.; Jemy, C.A. The effect of rainfall on slope failure, with examples from the Greater Durban area. In Proceedings of the 7th international Congress IAEG, Lisboa, Portugal, 5–9 September 1994; Volume 3, pp. 1629–1636.
17. Oh, K.D.; Hong, I.P.; Jun, B.H.; Ahn, W.S.; Lee, M.Y. Evaluation of gis-based landslide hazard mapping. *J. Korea Water Resour. Assoc.* **2006**, *39*, 23–33. (In Korean with English Abstract)
18. Cha, A. A comparison on the identification of landslide hazard using geomorphological characteristics. *J. Korean Geo-Environ. Soc.* **2014**, *15*, 67–73. (In Korean with English Abstract) [[CrossRef](#)]
19. Chae, B.-G.; Choi, J.; Heong, H.K. A feasibility study of a rainfall triggering index model to warn landslides in Korea. *J. Eng. Geol.* **2016**, *26*, 235–250. (In Korean with English Abstract) [[CrossRef](#)]
20. Hutchinson, J.N. Morphological and geotechnical parameters of landslides in relation to geology and hydrology. In Proceedings of the Landslides Fifth International Symposium on Landslides, Lausanne, Switzerland, 10–15 July 1988; Volume 1, pp. 3–35.
21. Kwak, J.H.; Kim, M.-I.; Lee, S.-J. Landslide susceptibility assessment considering the saturation depth ratio by rainfall change. *J. Eng. Geol.* **2018**, *28*, 687–699. (In Korean with English Abstract)
22. Highland, L.; Johnson, M. *Landslide Types and Processes*; Fact Sheet 2004-3072; USGS: Reston, VA, USA, 2004; 40p.
23. Lu, N.; Godt, J. Infinite-slope Stability under Steady Unsaturated Seepage Conditions. *Water Resour. Res.* **2008**, *44*, 1–13. [[CrossRef](#)]
24. Lee, S.; Jeong, G.; Park, S.J. Evaluating geomorphological classification systems to predict the occurrence of landslides in mountainous region. *J. Korean Geogr. Soc.* **2015**, *50*, 485–503. (In Korean with English Abstract)
25. Scarpelli, G.; Segato, D.; Sakellariadi, E.; Vita, A.; Ruggeri, P.; Fruzzetti, V.M.E. Slope Instability Problems in the Jonica Highway Construction. In Proceedings of the Second World Landslide Forum, Rome, Italy, 3–9 October 2011; pp. 1–6.
26. Sewell, R.J.; Fletcher, C.J.N. *Pilot Study on Regolith Mapping in Hong Kong*; Geological Report GR 1/2000; GEO: Nagoya, Japan, 2000; 45p.
27. Lepore, C.; Kamal, S.A.; Shanahan, P.; Bras, R.L. Rainfall-induced landslide susceptibility zonation of Puerto Rico. *Environ. Earth Sci.* **2012**, *66*, 1667–1681. [[CrossRef](#)]
28. Olivares, L.; Picarelli, L. Shallow flowslides triggered by intense rainfalls in natural slopes covered by loose unsaturated pyroclastic soils. *Geotechnique* **2003**, *53*, 283–287. [[CrossRef](#)]
29. Springman, S.M.; Jommi, C.; Teyssere, P. Instability on moraine slopes induced by loss of suction: A case history. *Geotechnique* **2003**, *53*, 3–10. [[CrossRef](#)]
30. Xue, J.; Gavin, K. Effect of rainfall intensity on infiltration into partly saturated slopes. *Geotech. Geol. Eng.* **2008**, *26*, 199–209. [[CrossRef](#)]
31. Rahardjo, H.; Leong, E.C.; Rezaur, R.B. Effect of antecedent rainfall on pore-water pressure distribution characteristics in residual soil slopes under tropical rainfall. *Hydrol. Process.* **2008**, *22*, 506–523. [[CrossRef](#)]
32. Ering, P.; Sivakumar Babu, G.L. Probabilistic back analysis of rainfall-induced landslide—A case study of Malin landslide, India. *Eng. Geol.* **2016**, *208*, 154–164. [[CrossRef](#)]
33. Fredlund, D.G.; Xing, A.; Huang, S. Predicting the permeability function for unsaturated soils using the soil-water characteristic curve. *Can. Geotech. J.* **1994**, *31*, 533–546. [[CrossRef](#)]
34. Fourie, A.B.; Rowe, D.; Blight, G.E. The effect of infiltration on the stability of the slopes of a dry ash dump. *Geotechnique* **1999**, *49*, 1–13. [[CrossRef](#)]
35. Rahardjo, H.; Li, X.E.; Toll, D.G.; Leong, E.C. The effect of antecedent rainfall on slope stability. *Geotech. Geol. Eng.* **2001**, *19*, 371–399. [[CrossRef](#)]
36. Lee, S.R.; Oh, T.K.; Kim, Y.K.; Kim, H.C. Influence of Rainfall Intensity and Saturated Permeability on Slope Stability during Rainfall Infiltration. *J. Korean Geotech. Soc.* **2009**, *25*, 65–76. (In Korean with English Abstract)
37. Korean Standards Association. *Standard Test Method for Particle Size Distribution of Soils*; KS F 2302; Korean Standards Association: Seoul, Korea, 2017.

38. Korean Standards Association. *Standard Test Method for Water Content of Soils*; KS F 2306; Korean Standards Association: Seoul, Korea, 2015.
39. Korean Standards Association. *Standard Test Method for Density of Soil Particles*; KS F 2308; Korean Standards Association: Seoul, Korea, 2016.
40. Korean Standards Association. *Standard Test Method for Density of Soil in Place by the Sand cone Method*; KS F 2311; Korean Standards Association: Seoul, Korea, 2016.
41. Korean Standards Association. *Standard Test Method for Permeability of Saturated Soils*; KS F 2322; Korean Standards Association: Seoul, Korea, 2015.
42. Cho, S.E.; Lee, S.R. Slope stability analysis of unsaturated soil slopes due to rainfall infiltration. *J. Korean Geotech. Soc.* **2000**, *16*, 51–64. (In Korean with English Abstract)
43. Kim, J.H.; Jeong, S.S.; Regueiro, R.A. Instability of partially saturated soil slopes due to alteration of rainfall pattern. *Eng. Geol.* **2012**, *147–148*, 28–36. [[CrossRef](#)]
44. Alyamani, M.S.; Sen, Z. Determination of hydraulic conductivity from grain size distribution curves. *Ground Water* **1993**, *31*, 551–555. [[CrossRef](#)]
45. Odong, J. Evaluation of empirical formulae for determination of hydraulic conductivity based on grain-size analysis. *J. Am. Sci.* **2008**, *4*, 1–6.
46. Nagy, L.S. Permeability of well graded soils. *Period. Polytech. Civ. Eng.* **2011**, *55*, 199–204. [[CrossRef](#)]
47. Singh, A.; Noor, S. Estimation of soil permeability using soil index properties. *Int. J. Latest Trends Eng. Technol.* **2012**, *1*, 31–33.
48. Elhakim, A.F. Estimation of soil permeability. *Alex. Eng. J.* **2016**, *55*, 2631–2638. [[CrossRef](#)]
49. Hazen, A. *Some Physical Properties of Sands and Gravels, with Special Reference to their Use in Filtration*; 24th Annual Report; Massachusetts State Board of Health: Boston, MA, USA, 1892; Volume 34, pp. 539–556.
50. Carrier, W.D. Goodbye, Hazen; Hello, Kozeny-Carman. *J. Geotech. Geoenviron. Eng.* **2003**, *129*, 1054–1056. [[CrossRef](#)]
51. Holtz, R.D.; Kovacks, W.D. *An Introduction to Geotechnical Engineering*; Prentice-Hall: Upper Saddle River, NJ, USA, 1981; 733p.
52. Hamidi, A.; Azini, E.; Masoudi, B. Impact of gradation on the shear strength-dilation behavior of well-graded sand-gravel mixtures. *Sci. Iran. A* **2012**, *19*, 393–402. [[CrossRef](#)]
53. Kolbuszewski, J.; Frederick, M.R. The significance of particle shape and size on the mechanical behavior of granular materials. In Proceedings of the European Conference on Soil Mechanics and Foundation Engineering, Wiesbaden, Germany, 15–18 October 1963; Volume 4, pp. 253–263.
54. Chattopadhyaya, B.C.; Saha, S. Effect of grain size of cohesionless soil on its shear strength characteristics. In Proceedings of the Geomech 81: Proceeding Symposium on Engineering Behaviour of Coarse Grained Soils, Boulders and Rocks, Hyderabad, India, 21–23 December 1981; Volume 1, pp. 291–297.
55. Sitharam, G.T.; Nimbkar, S.M. Micromechanical Modelling of Granular Materials: Effect of Particle Size and Gradation. *Geotech. Geol. Eng.* **2000**, *18*, 91–117. [[CrossRef](#)]
56. Katzenbach, R.; Schmitt, A. Micromechanical modelling of granular materials under triaxial and oedometric loading. In *Numerical Modeling in Micromechanics via Particle Methods-2004-Shimizu*; Shimizu, Y., Hart, R., Cundall, P., Eds.; CRC Press: London, UK, 2004; pp. 313–322.
57. Arkkelin, D. Using SPSS to understand research and data analysis. In *Psychology Curricular Materials*; Book 1; Valparaiso University: Valparaiso, Indiana, 2014; 194p. Available online: http://scholar.valpo.edu/psych_oer/1 (accessed on 2 May 2020).
58. Wang, Q.; Wang, W.; He, X.; Zheng, Q.; Wang, H.; Wu, Y.; Zhong, Z. Changes in soil properties, X-ray-mineral diffractions and infrared-functional groups in bulk soil and fractions following afforestation of farmland, Northeast China. *Sci. Rep.* **2017**, *7*, 12829. [[CrossRef](#)]
59. Griffiths, J.S.; Hearn, G.J. Engineering geomorphology: A UK perspective. *Bull. Int. Assoc. Eng. Geol.* **1990**, *42*, 39–44. [[CrossRef](#)]
60. Kim, W.-Y.; Chae, B.-G. Characteristics of rainfall, geology and failure geometry of the landslide areas on natural terrains, Korea. *J. Eng. Geol.* **2009**, *19*, 331–344. (In Korean with English Abstract)
61. Hungr, O.; Leroueil, S.; Picarelli, L. The Varnes classification of landslide types, an update. *Landslides* **2014**. [[CrossRef](#)]

62. Giannecchini, R.; Pochini, A. Geotechnical influence on soil slips in the Apuan Alps (Tuscany): First results in the Cardoso area. In Proceedings of the International Conference on Fast Movements-Prediction and Prevention for Risk Mitigation (IC-FSM 2003), Naples, Italy, 11–13 May 2003; pp. 241–245.
63. Gallage, C.P.K.; Uchimura, T. Effects of dry density and grain size distribution on soil-water characteristic curves of sandy soils. *Soils Found.* **2010**, *50*, 161–172. [[CrossRef](#)]



© 2020 by the authors. Licensee MDPI, Basel, Switzerland. This article is an open access article distributed under the terms and conditions of the Creative Commons Attribution (CC BY) license (<http://creativecommons.org/licenses/by/4.0/>).